CIRP Annals - Manufacturing Technology 63 (2014) 465–468

Contents lists available at ScienceDirect

CIRP Annals - Manufacturing Technology

journal homepage: http://ees.elsevier.com/cirp/default.asp

A novel dark field in-process optical inspection method for micro-openings on mirrored surfaces beyond the diffraction limit using active phase control

S. Takahashi (2)[a,*], H. Yokozeki[a], D. Fujii[b], R. Kudo[c], K. Takamasu[a]

[a] Department of Precision Engineering, The University of Tokyo, Hongo 7-3-1, Bunkyo-ku, Tokyo 113-8656, Japan
[b] Development Headquarters, Precision Equipment Company, Nikon Corporation, Miizugahara 201-9, Kumagaya-shi, Saitama 360-8559, Japan
[c] Research Center for Ultra-Precision Science and Technology, Osaka University, Yamadaoka 2-1, Suita-shi, Osaka 565-0861, Japan

ARTICLE INFO

Keywords:
Inspection
Optical
Nanostructure

ABSTRACT

We propose a novel in-process optical inspection method for micro-openings on a mirrored surface, such as mechanical functional gaps in micro-electro-mechanical systems (MEMS) and microchannels in microfluidics systems. The proposed method has not only highly sensitive detection characteristics based on dark field observations but also super-resolution observation characteristics based on the light scattering dependence of the edges of the micro-opening on the orientation of incident light under coherent imaging. Both theoretical and experimental analyses suggest that we can confirm the existence of proper micro-openings beyond the diffraction limit of imaging optics by shifting the relative phase of the counter-propagating incident beams.

1. Introduction

Micro-fabricated devices such as micro-electro-mechanical systems (MEMS) and microfluidics systems have recently attracted attention due to their specialized functionalities, which are characterized by their miniaturized structure [1–3]. In order to reliably fabricate these devices, in-process quality control methods based on nano- or micro-metrology are gaining importance [4–11].

Of the various in-process quality control factors for evaluating microstructures, one of the most important inspection factors is a micro-opening on the surface. Two typical micro-openings, shown in Fig. 1, are mechanical functional gaps in MEMS and microchannels in microfluidics systems. The lack of such micro-openings may cause functionality problems in the final products, such as the dynamic mechanical characteristics of microbeams in MEMS sensors. Therefore, one of the most important targets of in-process quality control for micro-functional devices is the verification of proper micro-openings on the device surface. Fig. 2 shows examples of defective micro-openings, which we must detect to ensure proper functionality of the final device.

There are several inspection techniques that allow us to confirm the existence of proper micro-openings, which are based on various measurement principles such as scanning electron microscopy (SEM), atomic force microscopy (AFM), optical-based microscopy, and so on [5]. Among these, optical techniques have a high affinity for in-process inspection and are superior because they are non-invasive. Furthermore, because optical techniques do not require a vacuum preparation or mechanical probe scanning, they are capable of high-throughput [7–12].

In optical techniques, dark field optical microscopy is well known as a highly sensitive inspection method for microscattering substances on the mirrored surface [13,14]. Fig. 3 shows a schematic diagram of conventional dark field optical inspection of micro-opening. Sharp edges on the surface opening, which indicate a proper gap, generate clear twin peaks in the intensity distribution of the microscopic optical system imaging plane (Fig. 3(a)). If an edge is defective or if a gap is closed due to an improper development process, less than two peaks appear in the intensity distribution (Fig. 3(b)). In this manner, highly sensitive detection

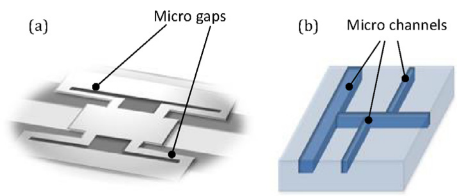

Fig. 1. Typical micro-openings on the mirrored surfaces of microfunctional devices such as (a) MEMS and (b) microfluidics devices.

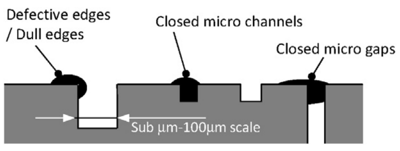

Fig. 2. Schematic diagram of typical defective micro-gaps and channels on surfaces, which are required to be detected.

* Corresponding author.

http://dx.doi.org/10.1016/j.cirp.2014.03.035
0007-8506/© 2014 CIRP.

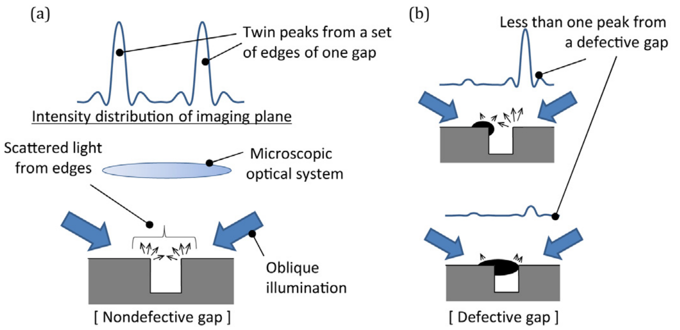

Fig. 3. Conventional dark field optical inspection of micro-opening. (a) Optical system and nondefective gap case. (b) Defective gap case.

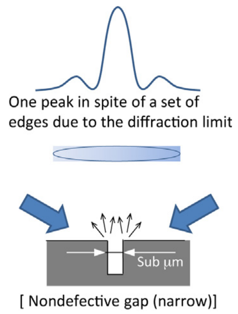

Fig. 4. Critical problem of conventional optical inspection due to the diffraction limit.

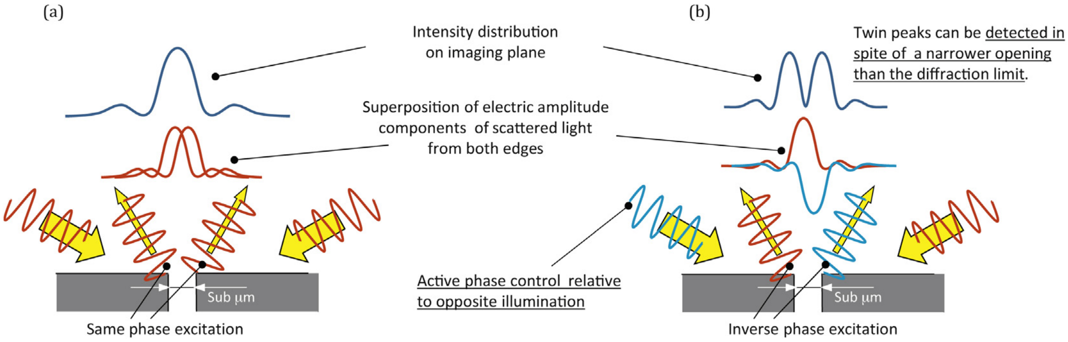

Fig. 5. Proposed dark field super-resolution optical inspection beyond the diffraction limit with active phase control under coherent conditions. (a) Same phase excitation case. (b) Inverse phase excitation case.

of micro-openings, which consist of a pair of fine scattering substances, is possible because the biased intensity corresponding to the specular reflection from the flat surface can be eliminated and only the scattered light from edges can be detected based on the fact that most surfaces with micro-openings behave like mirrored optical surfaces under dark field illumination.

Unfortunately, it is difficult to directly apply conventional dark field optical inspection to the next-generation manufacturing process of micro-fabricated devices, because minimal feature sizes of microstructures have been getting smaller to sub-micrometer scale, and which means that even nondefective micro-opening cannot generate clear twin peaks of the intensity distribution but only one peak especially when the gap width of the micro-opening is less than the diffraction limit of the optical system [12] as shown in Fig. 4. In order to overcome this problem, we propose a novel method for the dark field optical inspection of micro-openings using active phase control, which allows not only highly sensitive detection of the optical response of micro-opening edges but also super-resolution observation beyond the diffraction limit. In this study, we have theoretically and experimentally verified the feasibility of the proposed method.

2. Dark field optical inspection using active phase control

Fig. 5 shows the proposed super-resolution optical inspection method for micro-openings beyond the diffraction limit with active phase control under coherent conditions. In this proposed method, coherent laser beams, capable of interference, provide dark field oblique light illumination. In general, the detected optical image is formed by adding the optical images from light scattered light off the micro-opening edges, originating from one-sided oblique illumination on either side of the gap.

For a system under coherent conditions, optical superposition on the imaging plane is performed not with the intensity component but with the amplitude component of scattered light from the micro-opening. Because the light scattering at the edges depends on the incident light orientation, the phase of the amplitude distribution from one-sided oblique illumination can be changed by controlling the relative phase difference of the two counter-propagating illumination beams.

For micro-openings smaller than the diffraction limit, if the phase of the amplitude distribution is the same state, we obtain one peak of the intensity distribution, which is similar to conventional incoherent dark field inspection, as shown in Fig. 5(a). However, if the phase of the amplitude distribution is an inverse state, we expect clear twin peaks of the intensity distribution even for micro-openings smaller than the diffraction limit (Fig. 5(b)).

3. Numerical analyses of proposed concept

3.1. Simulation model and analysis of conventional method

In order to theoretically analyze optical imaging formed from micro-openings with a gap size on the order of the wavelength, the near-field optical interaction of the microstructures should be rigorously considered [15]; therefore, we perform numerical simulations using a finite-difference time-domain (FDTD) method [16], where we can calculate the electric field vector components interacting with arbitrarily fine structures with nanometer-scale resolution. Fig. 6 shows the FDTD simulation model used in this research. The simulation region consisting of the 20-nm unit cells was 2 μm × 1 μm × 2.5 μm. For the external light illuminating the micro-opening on the silicon substrate, we used two oblique s-polarized incident plane waves with a 488.0-nm wavelength at an incident angle of 80°.

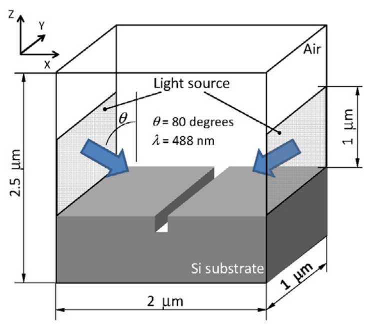

Fig. 6. FDTD simulation model for near-field optical response analyses.

Fig. 7 shows a typical optical response under conventional incoherent conditions, where two counter-propagating beams do not have any phase correlation. In this result, Fig. 7(a) shows the near-field intensity distribution on the XZ-plane for a 330-nm gap width. The mutual interaction at both edges of the micro-opening provides near-field light excitation at the center of the micro-opening. Fig. 7(b) shows the far-field intensity distribution on the imaging plane, which was calculated based on the Fourier optics from the complex amplitude distribution on the surface of the silicon substrate. Here, the numerical aperture (NA) of the optical system is assumed to be 0.9, resulting in a Rayleigh diffraction limit of 330 nm, which is equivalent to the gap width. In Fig. 7(b), only one peak of the intensity distribution is obtained even for a gap width of the Rayleigh diffraction limit because the edge opening is small compared with the wavelength.

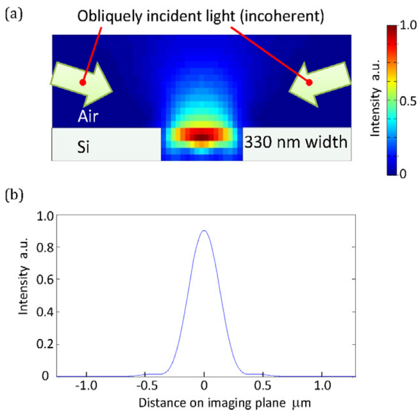

Fig. 7. Numerical result under conventional incoherent dark field inspection [XZ-plane] (Gap width: 330 nm). (a) Near-field intensity distribution. (b) Far-field intensity distribution on the imaging plane (*NA*: 0.9, Rayleigh diffraction limit: 330 nm).

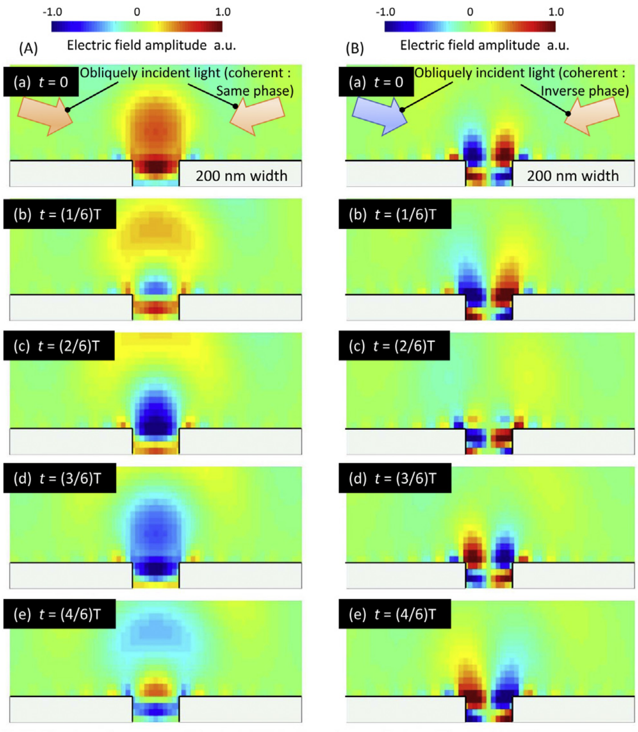

Fig. 8. Time-lapse images of the near-field excitation of the electric field component under the proposed coherent dark field inspection [XZ-plane] (Gap width: 200 nm). (A) Same phase excitation condition ($\phi = 0$). (B) Inverse phase excitation condition ($\phi = \pi$).

3.2. Analyses of the proposed method using active phase control

In order to verify the super-resolution of our proposed method, we analyze the optical response for gap widths smaller than the Rayleigh diffraction limit under the proposed coherent dark field inspection conditions. Fig. 8 shows time-lapse images of the near-field excitation of the electric field component for a 200-nm gap width where the Rayleigh diffraction limit is 330 nm. In Fig. 8(A), the counter-propagating illumination beams generate one near-field light peak from the electric dipoles at both edges in silicon substrate with same phase and the electromagnetic waves radiate upward. On the other hand, for the inverse phase excitation shown in Fig. 8(B), two near-field light peaks with different phases are observed near the micro-opening even if the gap is less than half of the wavelength.

Fig. 9 shows influence of the relative phase difference ϕ on the optical response under the same conditions. Fig. 9(A) and (B) respectively show the time-averaged near-field intensity distribution and far-field intensity distribution on the imaging plane with the same optical system as that in Fig. 7(b). From this, the 200-nm-gap can be clearly discerned with twin peaks of the intensity distribution on the far-field imaging plane by setting the relative phase difference $\phi = \pi$, even when the gap was less than the Rayleigh diffraction limit of the optical system.

Fig. 10 shows the gap discrimination characteristics of active phase control. As the NA decreases, the allowed relative phase

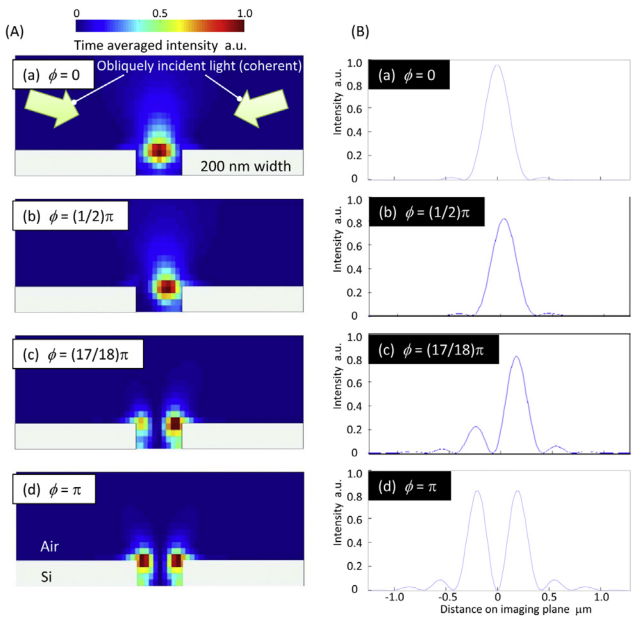

Fig. 9. Influence of relative phase difference ϕ on optical response under proposed coherent dark field inspection [XZ-plane] (Gap width: 200 nm). (A) Time-averaged near-field intensity distribution. (B) Far-field intensity distribution on the imaging plane (*NA*: 0.9, Rayleigh diffraction limit: 330 nm).

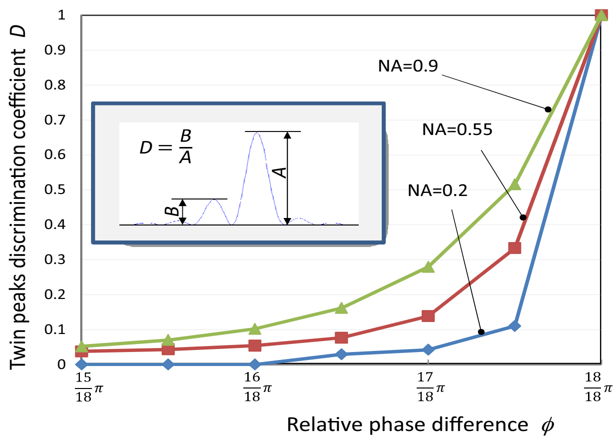

Fig. 10. Gap discrimination characteristics by controlling the relative phase difference ϕ (GAP width: 200 nm).

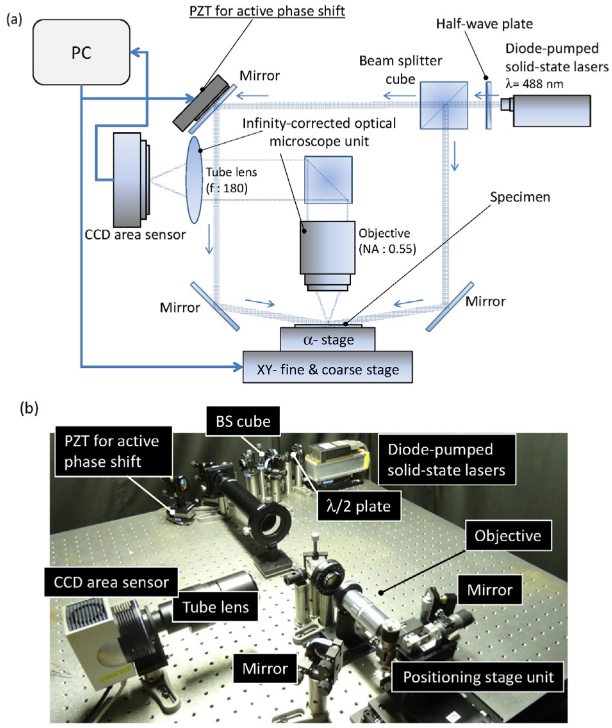

Fig. 11. Dark field optical inspection system with active phase control unit. (a) Schematic diagram. (b) Photograph of developed system.

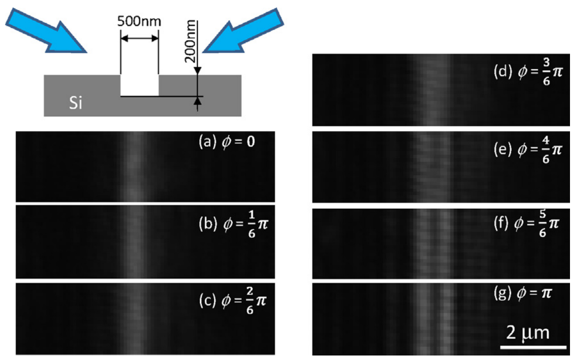

Fig. 12. Dark field observation images experimentally obtained using active phase control (Gap width: 500 nm, *NA*: 0.55, Rayleigh diffraction limit: 541 nm).

difference required for obtaining high contrast twin peaks decreases. However, for the relatively low NA of 0.2, where the Rayleigh diffraction limit is 1488 nm, the twin peaks of the intensity distribution on the far-field imaging plane can be obtained for a 200-nm gap by adjusting the relative phase difference. The effects of other detection parameters such as the incident angle on the quantitative gap width detection performance will be analyzed in a future work.

4. Fundamental experiments for verifying proposed concept

We developed a dark field optical inspection system with active phase control based on the proposed concept shown in Fig. 11. This experimental system consists of a continuous wave (CW) blue laser (Coherent, Sapphire LP 488-150, TEM00, M2 < 1.1) as a linearly polarized light source, a beam splitter cube generating two oblique counter-propagating incident beams, a piezoelectric translator with a mirror for shifting the relative phase difference of the two counter-propagating beams, an infinity-corrected optical microscope with a 16-bit cooled charge-coupled device (CCD) area sensor (Bitran BS-40), and a computer that controls the CCD, piezoelectric translator, and sample positioning stage.

To experimentally verify the proposed concept, we first conducted basic experiments for resolving a set of micro-opening edges with a 500-nm gap width on a silicon substrate using a relatively low NA objective (0.55). The Rayleigh diffraction limit under this condition was 541 nm. The other experimental conditions were as follows: wavelength $\lambda = 488$ nm, incident angle $\theta = 74°$, exposure time of 0.03 s, and microscope magnifying power of 90. The images in Fig. 12 correspond to the dark field observation images for the shifting relative phase difference of the counter-propagating beams, which is performed by moving the mirror on piezoelectric translator. Here, the phase difference values are relatively indicated from one peak image with the highest contrast (Fig. 12(a)). We clearly confirmed the 500-nm-gap with clear twin peaks of the intensity distribution beyond the Rayleigh diffraction limit (541 nm) by shifting the relative phase difference ϕ. This confirms our theoretically derived results.

5. Conclusions

We proposed a novel dark field optical inspection method, which allows us to confirm the existence of micro-openings with gap widths less than the diffraction limit of the imaging optics. The system is based on both the coherent imaging characteristics and the light scattering dependence of edges on the orientation of incident light under dark field observation. Theoretical analyses indicate that two near field light peaks originated from both edges of micro-opening can generate even in the narrower space (200 nm) compared with wavelength of light source (488 nm) by adjusting the relative phase difference of the oblique counter-propagating incident beams and clear twin peaks of the intensity distribution on the imaging plane can be achieved by optical system with the Rayleigh diffraction limit of 330 nm. Furthermore, fundamental experiments verify our proposed concept clearly discerning a 500-nm-gap with a relatively low NA objective of 0.55 with a Rayleigh diffraction limit of 541 nm. In the future, we plan to develop detailed analyses for studying the quantitative gap width and the minimum detectable gap width.

References

[1] Masuzawa T (2000) State of the Art of Micromachining. *Annals of CIRP* 49(2):473–488.
[2] Van Brussel H, Peirs J, Reynaerts D, Delchambre A, Reinhart G, Roth N, Weck M, Zussman E (2000) Assembly of Microsystems. *Annals of CIRP* 49(2):451–472.
[3] Duffy DC, McDonald JC, Schueller OJA, Whitesides GM (1998) Rapid Prototyping of Microfluidic Systems in Poly(dimethylsiloxane). *Analytical Chemistry* 70:4974–4984.
[4] Kim B, Shcmittdiel MC, Degertekin FL, Kurfess TR (2004) Scanning Grating Microinterferometer for MEMS Metrology. *ASME Journal of Manufacturing Science and Engineering* 126(4):807–812.
[5] Hansen HN, Carneiro K, Haitjema H, De Chiffre L (2006) Dimensional Micro and Nano Metrology. *Annals of CIRP* 55(2):721–743.
[6] Jiang X, Whitehouse D (2006) Miniaturized Optical Measurement Methods for Surface Nanometrology. *Annals of CIRP* 55(1):577–580.
[7] Takahashi S, Miyoshi T, Takaya Y, Saito K (1998) In-Process Measurement Method for Detection and Discrimination of Silicon Wafer Surface Defects by Laser Scattered Defect Pattern. *Annals of CIRP* 47(1):459–462.
[8] Takahashi S, Kudo R, Usuki S, Takamasu K (2011) Super Resolution Optical Measurements of Nanodefects on Si Wafer Surface using Infrared Standing Evanescent Wave. *Annals of CIRP* 60(1):523–526.
[9] Persson U (1998) In-Process Measurement of Surface Roughness using Light Scattering. *Wear* 215:54–58.
[10] You J, Kim SW (2008) Optical Inspection of Complex Patterns of Microelectronics Products. *Annals of CIRP* 57(1):505–508.
[11] Lonardo PM, Bruzzone AA, Gambaro C (1991) Surface Characterization and Defect Detection by Analysis of Images Obtained with Coherent Light. *Annals of CIRP* 40(1):541–544.
[12] Hocken RJ, Chakraborty N, Brown C (2005) Optical Metrology of Surfaces. *Annals of CIRP* 54(2):169–183.
[13] Sanz JLC, Merkle F, Wong KY (1985) Automated Digital Visual Inspection with Dark-Field Microscopy. *Journal of the Optical Society of America A* 2(11):1857–1862.
[14] Terasawa T, Tezuka Y, Ito M, Tomie T (2004) High Speed Actinic EUV Mask Blank Inspection with Dark-Field Imaging. *Proceedings of SPIE* 5446:804–811.
[15] Mayes TW, Riley MS, Edward K, Fesperman R, Suraktar A, Shahid U, Williams S (2004) Phase Imaging in the Near Field. *Annals of CIRP* 53(1):483–486.
[16] Yee KS (1966) Numerical Solution of Initial Boundary Value Problems Involving Maxwell's Equations in Isotropic Media. *IEEE Transactions on Antennas and Propagation* 14(3):302–307.